Journal of Sound and Vibration (1987) 113(3), 503-527

ENTRAINED OSCILLATIONS IN A SYSTEM OF MUTUALLY COUPLED VAN DER POL OSCILLATORS WITH TIME DELAY IN THE COUPLING PATHS

A. KOUDA

Faculty of General Education, Tokyo University of Agriculture and Technology, 2-24 Naka-Machi, Koganei-Shi, Tokyo 184, *Japan*

AND

S. MORI

Department of Electrical Engineering, Keio University, 3-14-1 Hiyoshi, Kohoku-Ku, Yokohama 223, *Japan*

(*Received* 17 *October* 1984, *and in revised form* 9 *April* 1986)

A system of four mutually coupled van der Pol oscillators with time delay in the coupling paths is analyzed. The intrinsic (i.e., uncoupled) frequencies of these oscillators are given by $\omega_{0k} = 1 + \Delta\omega(k-1)$, $k = 1, 2, 3, 4$, where k denotes four oscillators and $\Delta\omega$ is the intrinsic frequency gradient. In this paper, it is shown that the coupling time delay, coupling factor, and gradient of intrinsic frequencies of such a system radically affect the number, frequency, amplitudes, and phases of entrained oscillations.

1. INTRODUCTION

The study of mutually coupled non-linear oscillators has received much attention in several fields of engineering, statistical mechanics, electronics, and biological science and has been discussed in numerous experimental and theoretical works [1-13]. In many of these works it has been assumed that the signals of the interaction between the partial oscillators are instantaneously transmitted without delay. However, in practice one often encounters cases in which the interconnected oscillators are located certain distances apart from each other, so that a certain amount of time τ is required for the passage of the interaction signal from one oscillator to another. Consequently, it is of definite interest to consider the effects of coupling delay on the processes of the interaction of oscillators. Systems of mutually coupled non-linear oscillators with a coupling delay have been investigated by several authors [14-19].

In this paper we analyze a system of four mutually coupled van der Pol oscillators with time delay in the coupling paths, which is described by four second order differential-difference equations (see Figure 1)

$$\ddot{\mathbf{x}} - \varepsilon(\mathbf{I} - \chi^2)\dot{\mathbf{x}} + \omega_0^2\mathbf{x} = \alpha\mathbf{B}\mathbf{x}_\tau, \tag{1}$$

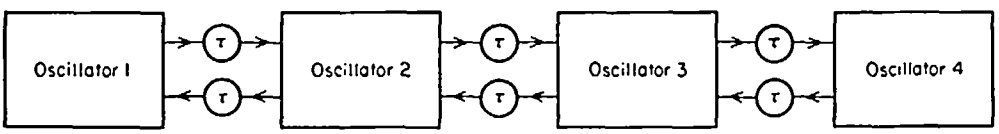

Figure 1. Block diagram for system (1).

where

$$\mathbf{x}=\begin{bmatrix}x_1\\x_2\\x_3\\x_4\end{bmatrix},\quad \mathbf{x}_\tau=\begin{bmatrix}x_1(t-\tau)\\x_2(t-\tau)\\x_3(t-\tau)\\x_4(t-\tau)\end{bmatrix},\quad \chi=\begin{bmatrix}x_1&&&0\\&x_2&&\\&&x_3&\\0&&&x_4\end{bmatrix},\quad \mathbf{I}=\text{unit matrix},$$

$$\omega_0=\begin{bmatrix}\omega_{01}&&&\\&\omega_{02}&&0\\&&\omega_{03}&\\&0&&\omega_{04}\end{bmatrix},\quad \mathbf{B}=\begin{bmatrix}0&1&0&0\\1&0&1&0\\0&1&0&1\\0&0&1&0\end{bmatrix}.$$

Dots represent differentiation with respect to time, x_k $(k=1,2,3,4)$ is the output (time series solution) of the kth van der Pol oscillator, ω_{0k} $(=1+\Delta\omega(k-1),\ k=1,2,3,4)$ is the intrinsic frequency of that oscillator, $\Delta\omega$ is the intrinsic frequency gradient, ε is the waveshape parameter (a small positive constant, $\varepsilon \ll 1$), α is the coupling factor (also a small positive constant), τ is the delay time (a positive constant), and $\mathbf{B}$ is a real, symmetric matrix of order four, representing the interaction links among the oscillators.

In biological applications, a chain of loosely coupled relaxation oscillators has been considered as an idealized model of the gastro-intestinal tract or the ureter, so system (1) may be also used as a subunit of a larger model in intestinal modeling.

Sinusoidal solutions of equation (1) have been found by using the method of harmonic balance [20]. The results obtained are compared with those provided by digital computer studies (digital simulations).

2. ANALYSIS

2.1. DETERMINATION OF ENTRAINED FREQUENCY, AMPLITUDES AND PHASES OF THE ENTRAINED OSCILLATION

An entrained solution of the form

$$x_k = A_k \sin(\omega t+\theta_k),\qquad k=1,2,3,4, \tag{2}$$

is assumed, where ω is the entrained frequency, A_k are the entrained amplitudes, and θ_k are the entrained phases (ω, A_k, and θ_k are constants to be determined). By substituting the solutions (2) and their time derivatives into equation (1), ignoring higher order terms in 3ω, and balancing coefficients of $\sin(\omega t+\theta_k)$ and $\cos(\omega t+\theta_k)$ on both sides, one can obtain the following eight algebraic relationships:

$$A_1(\omega_{01}^2-\omega^2)-\alpha A_2\cos(\theta_2-\theta_1-\omega\tau)=s_1=0, \tag{3a}$$

$$A_2(\omega_{02}^2-\omega^2)-\alpha A_1\cos(\theta_1-\theta_2-\omega\tau)-\alpha A_3\cos(\theta_3-\theta_2-\omega\tau)=s_2=0, \tag{3b}$$

$$A_3(\omega_{03}^2-\omega^2)-\alpha A_2\cos(\theta_2-\theta_3-\omega\tau)-\alpha A_4\cos(\theta_4-\theta_3-\omega\tau)=s_3=0, \tag{3c}$$

$$A_4(\omega_{04}^2-\omega^2)-\alpha A_3\cos(\theta_3-\theta_4-\omega\tau)=s_4=0, \tag{3d}$$

$$\varepsilon\omega A_1(1-A_1^2/4)+\alpha A_2\sin(\theta_2-\theta_1-\omega\tau)=c_1=0, \tag{3e}$$

$$\varepsilon\omega A_2(1-A_2^2/4)+\alpha A_1\sin(\theta_1-\theta_2-\omega\tau)+\alpha A_3\sin(\theta_3-\theta_2-\omega\tau)=c_2=0, \tag{3f}$$

$$\varepsilon\omega A_3(1-A_3^2/4)+\alpha A_2\sin(\theta_2-\theta_3-\omega\tau)+\alpha A_4\sin(\theta_4-\theta_3-\omega\tau)=c_3=0, \tag{3g}$$

$$\varepsilon\omega A_4(1-A_4^2/4)+\alpha A_3\sin(\theta_3-\theta_4-\omega\tau)=c_4=0. \tag{3h}$$

By solving these non-linear algebraic equations, the eight quantities, i.e., ω, A_k $(k=1,2,3,4)$, and θ_k $(k=2,3,4$, with θ_1 arbitrary], are obtained.

2.2. STABILITY PROBLEM

The stability of these oscillations can be investigated by considering the dynamic response to small variations from these oscillations. Equation (2) can be modified by allowing for small variations in amplitude and phase of each oscillator as follows:

$$x_k = (A_k + a_k)\sin(\omega t + \theta_k + \varphi_k), \qquad k = 1, 2, 3, 4, \tag{4}$$

where a_k and φ_k are functions of time t and these values are sufficiently small. If all these variations a_k and φ_k tend to zero with increasing t, the corresponding entrained oscillation is stable; if all or some of these variations diverge, this oscillation is unstable.

Equation (4) is easily expanded to the form

$$\begin{aligned} x_k = {} & A_k \cos\varphi_k \sin(\omega t + \theta_k) + a_k \cos\varphi_k \sin(\omega t + \theta_k) \\ & + A_k \sin\varphi_k \cos(\omega t + \theta_k) + a_k \sin\varphi_k \cos(\omega t + \theta_k), \qquad k = 1, 2, 3, 4. \end{aligned} \tag{5}$$

If φ_k $(k = 1, 2, 3, 4)$ is sufficiently small, the results are $\cos\varphi_k \doteqdot 1$ and $\sin\varphi_k \doteqdot \varphi_k$ $(k = 1, 2, 3, 4)$. Hence x_k can be rewritten as follows:

$$\begin{aligned} x_k = {} & A_k \sin(\omega t + \theta_k) + a_k \sin(\omega t + \theta_k) \\ & + A_k\varphi_k \cos(\omega t + \theta_k) + a_k\varphi_k \cos(\omega t + \theta_k), \qquad k = 1, 2, 3, 4. \end{aligned} \tag{6}$$

Neglecting the second order term, $a_k\varphi_k \cos(\omega t + \theta_k)$, $k = 1, 2, 3, 4$, one can write

$$\begin{aligned} x_k = {} & A_k \sin(\omega t + \theta_k) + \xi_k \sin(\omega t + \theta_k) \\ & + \eta_k \cos(\omega t + \theta_k), \qquad k = 1, 2, 3, 4, \end{aligned} \tag{7}$$

where $\xi_k = a_k$ and $\eta_k = A_k\varphi_k$. Substituting equation (7) into equation (1) and ignoring higher order terms in 3ω gives the variational equations:

$$\begin{aligned} & \ddot{\xi}_1 - \varepsilon(1 - \tfrac{3}{4}A_1^2)\dot{\xi}_1 + (\omega_{01}^2 - \omega^2)\xi_1 - 2\omega\dot{\eta}_1 + \varepsilon\omega(1 - \tfrac{1}{4}A_1^2)\eta_1 \\ & \quad - \alpha\cos(\theta_2 - \theta_1 - \omega\tau)\xi_{2\tau} + \alpha\sin(\theta_2 - \theta_1 - \omega\tau)\eta_{2\tau} = 0, \end{aligned} \tag{8a}$$

$$\begin{aligned} & 2\omega\dot{\xi}_1 - \varepsilon\omega(1 - \tfrac{3}{4}A_1^2)\xi_1 + \ddot{\eta}_1 - \varepsilon(1 - \tfrac{1}{4}A_1^2)\dot{\eta}_1 + (\omega_{01}^2 - \omega^2)\eta_1 \\ & \quad - \alpha\sin(\theta_2 - \theta_1 - \omega\tau)\xi_{2\tau} - \alpha\cos(\theta_2 - \theta_1 - \omega\tau)\eta_{2\tau} = 0, \end{aligned} \tag{8b}$$

$$\begin{aligned} & \ddot{\xi}_{k+1} - \varepsilon(1 - \tfrac{3}{4}A_{k+1}^2)\dot{\xi}_{k+1} + (\omega_{0k+1}^2 - \omega^2)\xi_{k+1} - 2\omega\dot{\eta}_{k+1} + \varepsilon\omega(1 - \tfrac{1}{4}A_{k+1}^2)\eta_{k+1} \\ & \quad - \alpha\cos(\theta_k - \theta_{k+1} - \omega\tau)\xi_{k\tau} + \alpha\sin(\theta_k - \theta_{k+1} - \omega\tau)\eta_{k\tau} \\ & \quad - \alpha\cos(\theta_{k+2} - \theta_{k+1} - \omega\tau)\xi_{k+2\tau} + \alpha\sin(\theta_{k+2} - \theta_{k+1} - \omega\tau)\eta_{k+2\tau} = 0, \end{aligned} \tag{8c}$$

$$\begin{aligned} & 2\omega\dot{\xi}_{k+1} - \varepsilon\omega(1 - \tfrac{3}{4}A_{k+1}^2)\xi_{k+1} + \ddot{\eta}_{k+1} - \varepsilon(1 - \tfrac{1}{4}A_{k+1}^2)\dot{\eta}_{k+1} + (\omega_{0k+1}^2 - \omega^2)\eta_{k+1} \\ & \quad - \alpha\sin(\theta_k - \theta_{k+1} - \omega\tau)\xi_{k\tau} - \alpha\cos(\theta_k - \theta_{k+1} - \omega\tau)\eta_{k\tau} \\ & \quad - \alpha\sin(\theta_{k+2} - \theta_{k+1} - \omega\tau)\xi_{k+2\tau} - \alpha\cos(\theta_{k+2} - \theta_{k+1} - \omega\tau)\eta_{k+2\tau} = 0, \qquad k = 1, 2, \end{aligned} \tag{8d}$$

$$\begin{aligned} & \ddot{\xi}_4 - \varepsilon(1 - \tfrac{3}{4}A_4^2)\dot{\xi}_4 + (\omega_{04}^2 - \omega^2)\xi_4 - 2\omega\dot{\eta}_4 + \varepsilon\omega(1 - \tfrac{1}{4}A_4^2)\eta_4 \\ & \quad - \alpha\cos(\theta_3 - \theta_4 - \omega\tau)\xi_{3\tau} + \alpha\sin(\theta_3 - \theta_4 - \omega\tau)\eta_{3\tau} = 0, \end{aligned} \tag{8e}$$

$$\begin{aligned} & 2\omega\dot{\xi}_4 - \varepsilon\omega(1 - \tfrac{3}{4}A_4^2)\xi_4 + \ddot{\eta}_4 - \varepsilon(1 - \tfrac{1}{4}A_4^2)\eta_4 + (\omega_{04}^2 - \omega^2)\eta_4 \\ & \quad - \alpha\sin(\theta_3 - \theta_4 - \omega\tau)\xi_{3\tau} - \alpha\cos(\theta_3 - \theta_4 - \omega\tau)\eta_{3\tau} = 0. \end{aligned} \tag{8f}$$

Here $\xi_{k\tau} = \xi_k(t - \tau)$ and $\eta_{k\tau} = \eta_k(t - \tau)$, $k = 1, 2, 3, 4$. When the substitutions $\xi_k \to \Xi_k\, e^{st}$ and $\eta_k \to H_k\, e^{st}$ (Ξ_k and H_k are constants) are made, the characteristic equation of the

variational equation (8) becomes as follows:†

$$D(s)=\begin{vmatrix} P_{11} & P_{12} & P_{13} & P_{14} & & & & \\ P_{21} & P_{22} & P_{23} & P_{24} & & & 0 & \\ P_{31} & P_{32} & P_{33} & P_{34} & P_{35} & P_{36} & & \\ P_{41} & P_{42} & P_{43} & P_{44} & P_{45} & P_{46} & & \\ & & P_{53} & P_{54} & P_{55} & P_{56} & P_{57} & P_{58} \\ & & P_{63} & P_{64} & P_{65} & P_{66} & P_{67} & P_{68} \\ & 0 & & & P_{75} & P_{76} & P_{77} & P_{78} \\ & & & & P_{85} & P_{86} & P_{87} & P_{88} \end{vmatrix}=0, \tag{9}$$

where

$$P_{2k-1,2k-1}=s^2-\varepsilon(1-\tfrac{3}{4}A_k^2)s+(\omega_{0k}^2-\omega^2), \qquad P_{2k-1,2k}=-2\omega s+\varepsilon\omega(1-\tfrac{1}{4}A_k^2),$$

$$P_{2k,2k-1}=2\omega s-\varepsilon\omega(1-\tfrac{3}{4}A_k^2), \qquad P_{2k,2k}=s^2-\varepsilon(1-\tfrac{1}{4}A_k^2)s+(\omega_{0k}^2-\omega^2), \qquad k=1,2,3,4,$$

$$P_{2k-1,2k+1}=P_{2k,2k+2}=-\alpha\,\mathrm{e}^{-\tau s}\cos(\theta_{k+1}-\theta_k-\omega\tau),$$

$$P_{2k-1,2k+2}=-P_{2k,2k+1}=\alpha\,\mathrm{e}^{-\tau s}\sin(\theta_{k+1}-\theta_k-\omega\tau),$$

$$P_{2k+1,2k-1}=P_{2k+2,2k}=-\alpha\,\mathrm{e}^{-\tau s}\cos(\theta_k-\theta_{k+1}-\omega\tau),$$

$$P_{2k+1,2k}=-P_{2k+2,2k-1}=\alpha\,\mathrm{e}^{-\tau s}\sin(\theta_k-\theta_{k+1}-\omega\tau), \qquad k=1,2,3.$$

Thus, the stability of the entrained oscillation can be determined by finding the locations of the roots of the characteristic equation (9) in the s-plane. The determination of the locations of these roots is carried out by making use of the Nyquist criterion [21]. Here, equation (9) is divided by $F_1(s)F_2(s)F_3(s)F_4(s)$, giving‡

$$D'(s)=D(s)/F_1(s)F_2(s)F_3(s)F_4(s), \tag{10}$$

where

$$F_k(s)=s^4+\varepsilon A_k^2 s^3+\{2(\omega_{0k}^2+\omega^2)+\varepsilon^2(1+\tfrac{3}{16}A_k^4)\}s^2$$
$$+\varepsilon(\omega_{0k}^2+\omega^2)A_k^2 s+(\omega_{0k}^2-\omega^2)^2+\varepsilon^2\omega^2(1+\tfrac{3}{16}A_k^4), \qquad k=1,2,3,4.$$

This is done since the limit of $D'(s)$ must approach a constant or zero (in equation (10)), when $s\to j\infty$ one has $D'(s)\to 1$ as s approaches ∞. So the stability of the corresponding oscillation can be determined by plotting the $D'(s)$ locus (s takes on values along the Nyquist path) and investigating the behavior of the $D'(s)$ plot with respect to the origin in the D'-plane. From the Nyquist criterion, the oscillation is stable, provided the Nyquist plot of $D'(s)$ does not encircle the origin.

3. NUMERICAL RESULTS

A numerical analysis has been carried out by using the waveshape parameter of 0·03 and the coupling factors of 0·2 and 0·3.

In the system being considered, there are four modes of entrained oscillation (because of the four-oscillator system). These oscillations were expressed as

$$x_{jk}=A_{jk}\sin(\omega_j t+\theta_{jk}), \tag{11}$$

† For $s=0$, $D(s)=0$.

‡ Since the poles of $D'(s)$ (i.e., zeros of $F_1(s)F_2(s)F_3(s)F_4(s)$) are all located in the left half of the s-plane, it is evident that there is no effect of these additional poles on the stability of the oscillation.

where j denotes four modes ($j=1,2,3,4$) and k four oscillators ($k=1,2,3,4$). The entrained frequencies ω_j, the entrained amplitudes A_{jk}, and the entrained phases θ_{jk}† have been found by solving equations (3a)-(3h). The problem of solving equations (3a)-(3h) can be replaced by the problem of minimizing the sum of the squares of the left-hand sides of these equations (i.e., $\sum_{n=1}^{4}(S_n^2+C_n^2)$). To solve this problem, the Newton-Raphson method ([22] and [23]) was used‡. By substituting the values obtained into equation (10), the stability of these oscillations (11) have been determined. An example of the practical application of the Nyquist criterion to determination of the stability of the oscillation is illustrated in Figure 2.

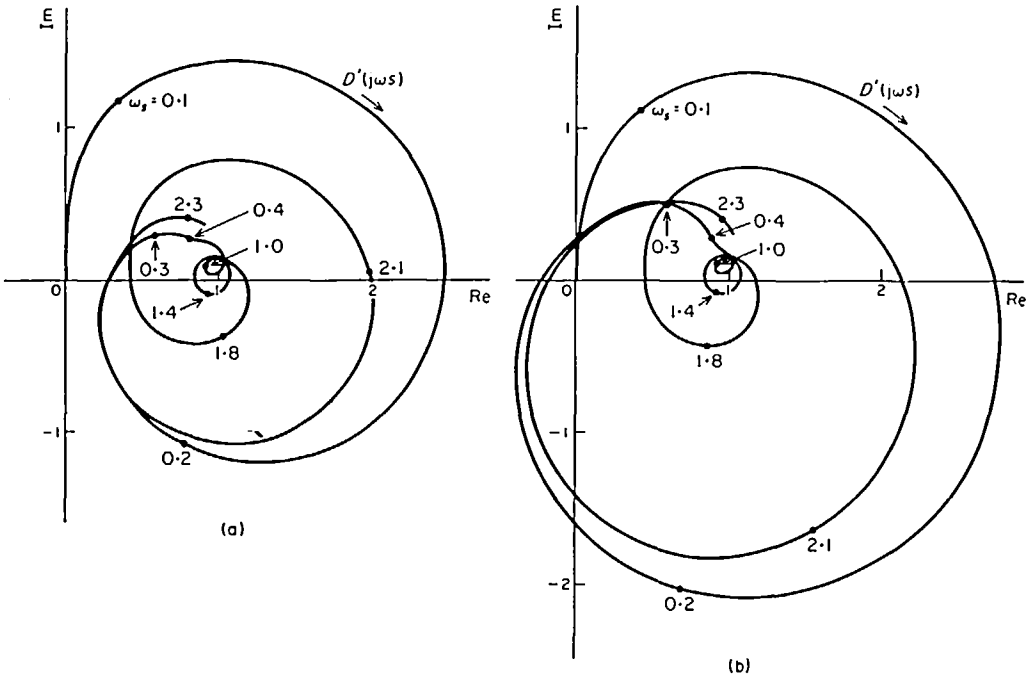

Figure 2. Example of the practical application of the Nyquist criterion to determining the stability of the entrained oscillations for $\Delta\omega = 0{\cdot}05$ and $\alpha = 0{\cdot}2$. (a) $\tau = 5{\cdot}6$ (in this case, since the origin is not enclosed by the Nyquist plot of $D'(s)$, the entrained oscillation is stable); (b) $\tau = 5{\cdot}8$ (for this value of time delay, the entrained oscillation is unstable).

Figures 3-6 show the variations of the entrained frequencies, entrained amplitudes, and entrained phases with increasing time delay for an intrinsic frequency gradient of zero. For very small values of time delay, four entrained oscillations are stable. Three of these oscillations (i.e., mode 1, mode 2, and mode 3) soon become unstable as τ increases. The details of these relationships between the stability of entrained oscillations and time delay are found in Table 1. In some intervals containing $\tau = n\pi$, $n=1,2,3,\ldots$, two entrained oscillations (i.e., mode 1 and mode 4) are stable; one of these oscillations is unstable for other values of τ. The regions in which two entrained oscillations are stable increase in size as τ (or the coupling factor α) increases. The regions of τ for which mode 1 is stable and those for which mode 4 is stable alternate as τ varies. Therefore, the phenomenon of discontinuous jumps in the mode of entrained oscillation occurs if

† Here the θ_{j1}'s ($j=1,2,3,4$) are taken equal to zero for simplicity, without loss of generality.

‡ Here the iteration for Newton's method is terminated when the value of $\sum_{n=1}^{4}(s_n^2+c_n^2)$ is less than a given value of 0·000001. The values obtained for ω_j, A_{jk} and θ_{jk} are reasonable.

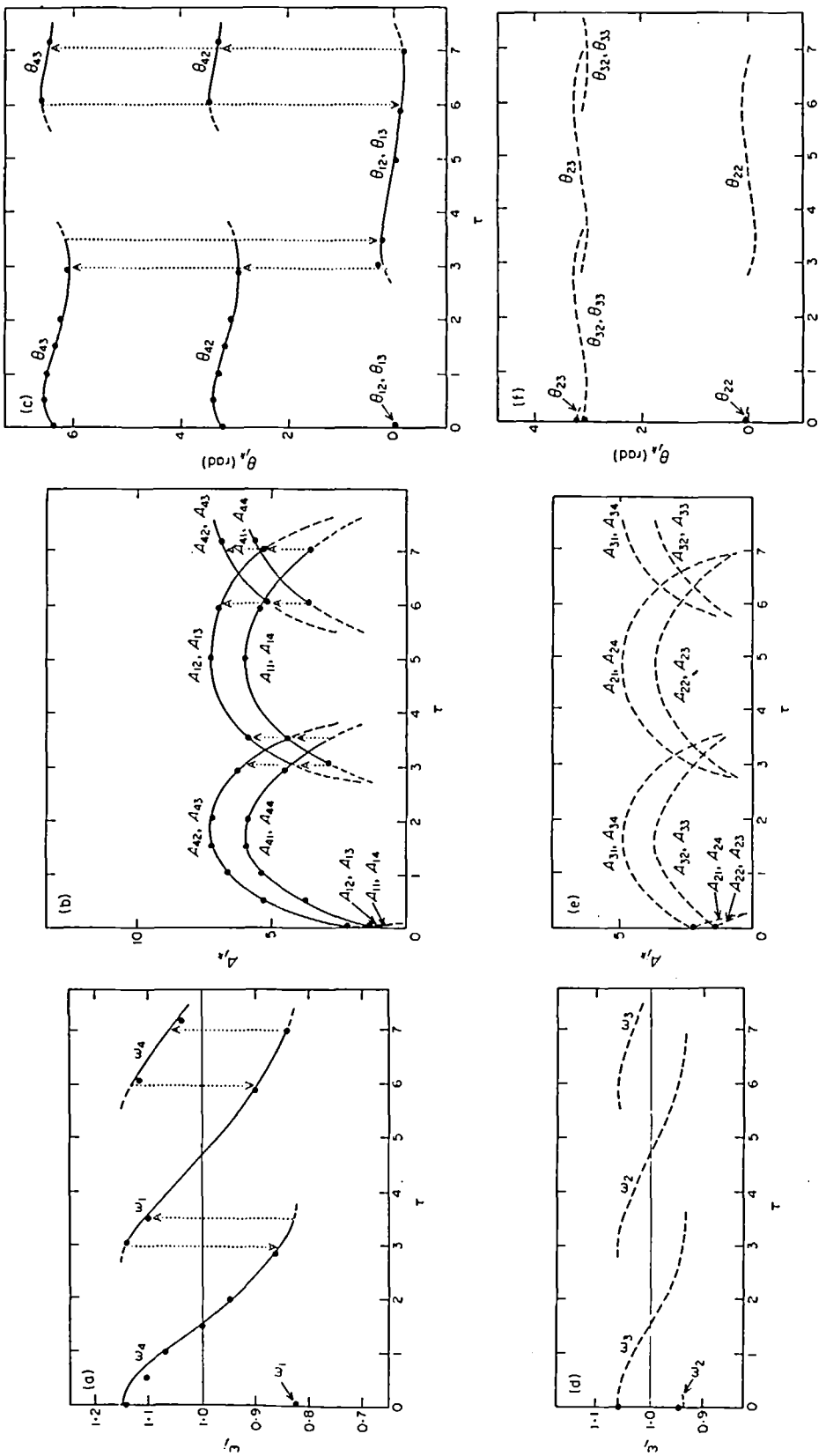

Figure 3. Variations of the entrained frequency ω_j, entrained amplitudes A_{jk}, and entrained phases θ_{jk} with time delay for $\Delta\omega = 0$ and $\alpha = 0{\cdot}2$. Note: In this and succeeding graphs ——, indicate stable modes (theoretical results), - - - - -, indicate unstable modes (theoretical results), and ●, indicate the results obtained by numerical integration. Vertical lines indicate the discontinuous jumps in the mode of the entrained oscillation. (a) ω_j of mode 1 and mode 4; (b) A_{jk} of mode 1 and mode 4; (c) θ_{jk} of mode 1 and mode 4 ($\theta_{11} = \theta_{41} = 0$, $\theta_{14} \doteqdot 0$, and $\theta_{44} \doteqdot 3\pi$); (d) ω_j of mode 2 and mode 3; (e) A_{jk} of mode 2 and mode 3; (f) θ_{jk} of mode 2 and mode 3 ($\theta_{21} = \theta_{31} = 0$, $\theta_{24} \doteqdot \pi$, and $\theta_{34} \doteqdot 2\pi$).

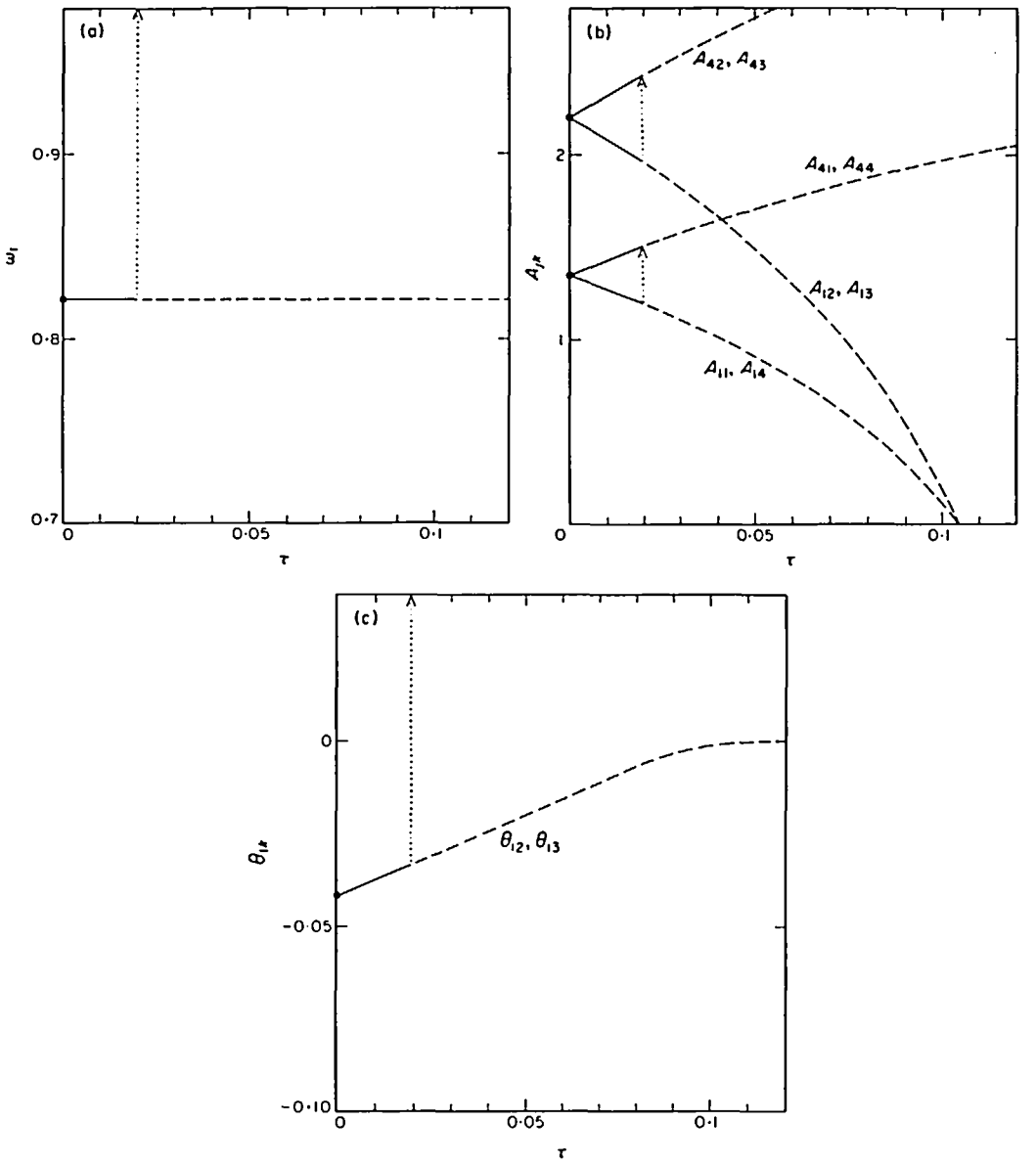

Figure 4. Expanded version of Figure 3 showing mode 1 for very small values of time delay. (a) Entrained frequency; (b) entrained amplitudes (A_{4k} are the entrained amplitudes of mode 4); (c) entrained phases ($\theta_{11} = 0$, $\theta_{14} \doteq 0$).

τ is varied smoothly and continuously. These jumps are indicated by vertical lines in Figures 3-6 (the jumps for $\Delta\omega = 0{\cdot}05$ are seen in Figures 8 and 9).

In Figures 7, 8 and 9 the variations of entrained frequencies, entrained amplitudes, and entrained phases with increasing time delay for intrinsic frequency gradient of 0·05, are shown. For $\alpha = 0{\cdot}2$, in some intervals containing $\tau = (n-1)\pi$, $n = 1, 2, 3, \ldots$, all the entrained oscillations are unstable. For other values of τ, only one entrained oscillation (mode 1 or mode 4) is stable. The regions of τ for which mode 1 is stable and those for which mode 4 is stable alternate as τ varies. The regions in which all the entrained

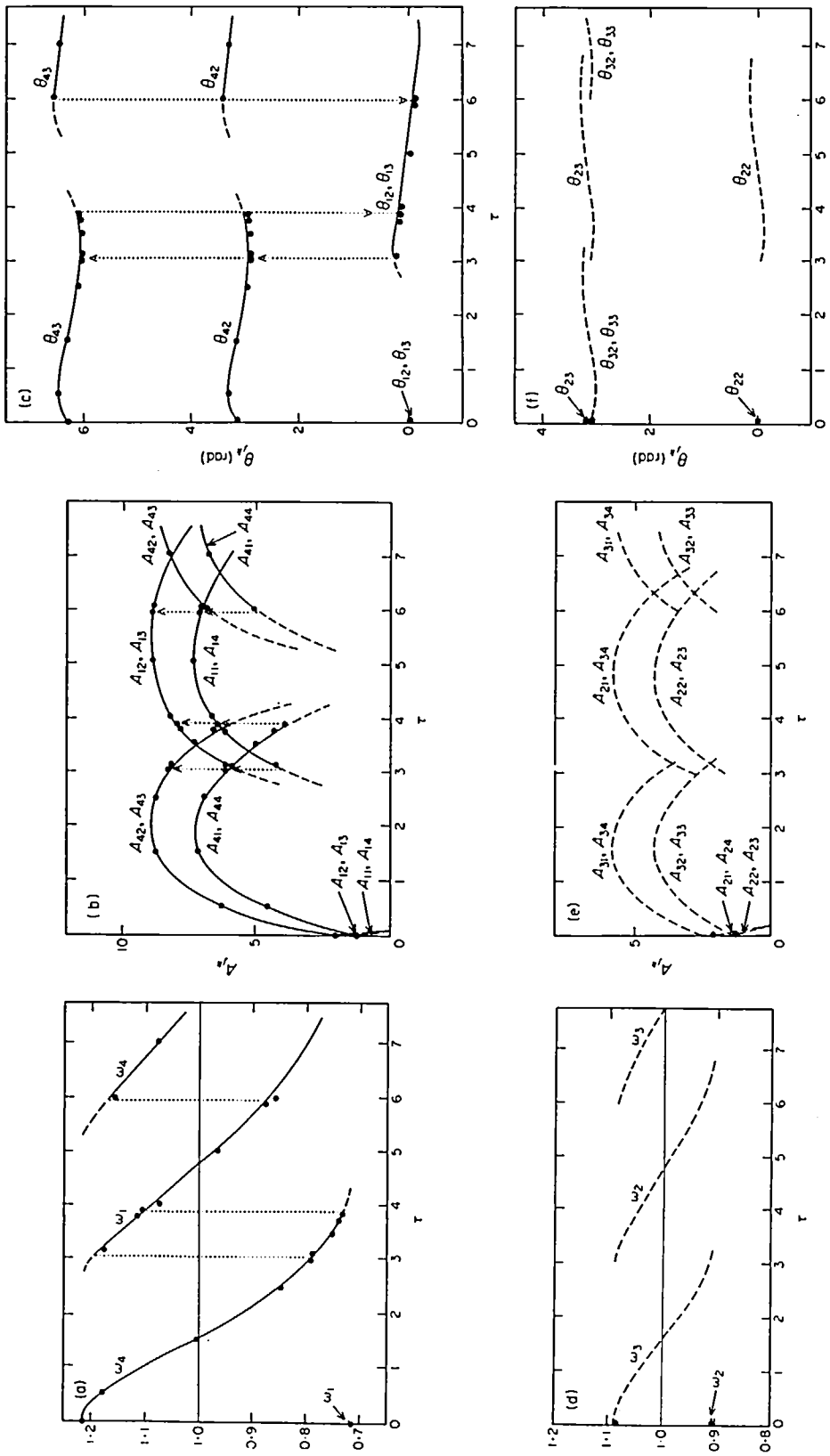

Figure 5. Variations of the entrained frequencies ω_j, entrained amplitudes A_{jk}, and entrained phases θ_{jk} with time delay for $\Delta\omega = 0$ and $\alpha = 0{\cdot}3$. (a) ω_j of mode 1 and mode 4; (b) A_{jk} of mode 1 and mode 4; (c) θ_{jk} of mode 1 and mode 4 ($\theta_{11} = \theta_{41} = 0$, $\theta_{14} \doteq 0$, and $\theta_{44} \doteq 3\pi$); (d) ω_j of mode 2 and mode 3; (e) A_{jk} of mode 2 and mode 3; (f) θ_{jk} of mode 2 and mode 3 ($\theta_{21} = \theta_{31} = 0$, $\theta_{24} \doteq \pi$, and $\theta_{34} \doteq 2\pi$).

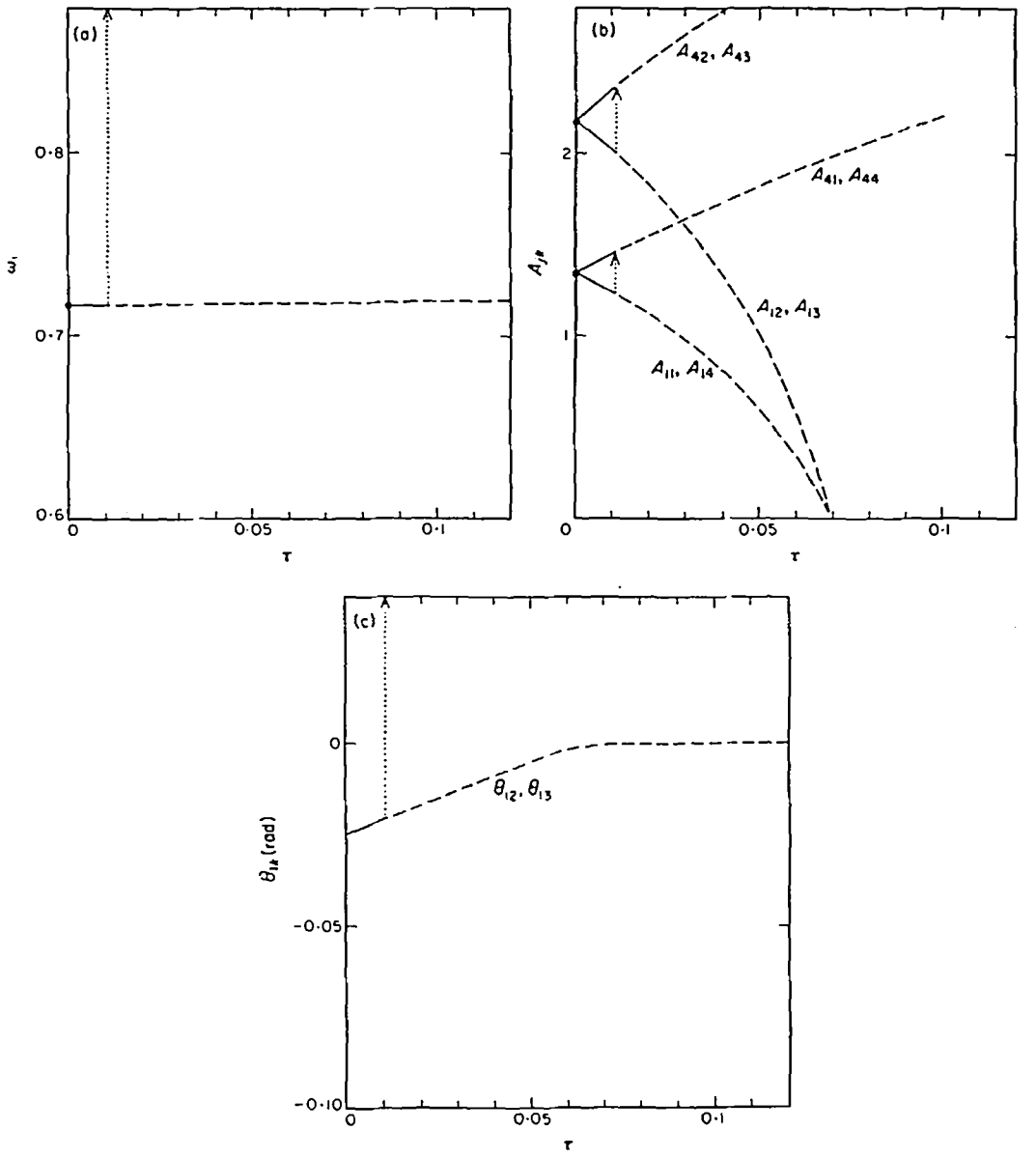

Figure 6. Expanded version of Figure 5 showing mode 1 for very small values of time delay. (a) Entrained frequency; (b) entrained amplitudes (A_{4k} are the entrained amplitudes of mode 4); (c) entrained phases ($\theta_{11} = 0$, $\theta_{14} \doteq 0$).

oscillations are unstable increase in size with increasing τ (these are shown by the dotted areas in Figure 7). As α increases these regions vanish, and the regions of τ for which the entrained oscillations are stable are obtained. The mode stabilities for very small values of τ are also shown in Table 2. It becomes clear from the above results that only for sufficiently small values of τ are mode 2 and mode 3 stable.

Figure 10 shows the variations of the entrained frequencies, entrained amplitudes, and entrained phases with increasing intrinsic frequency gradient for $\alpha = 0{\cdot}2$ and $\tau = 0$. From this figure it becomes clear that the entrained amplitudes, and entrained phases of mode

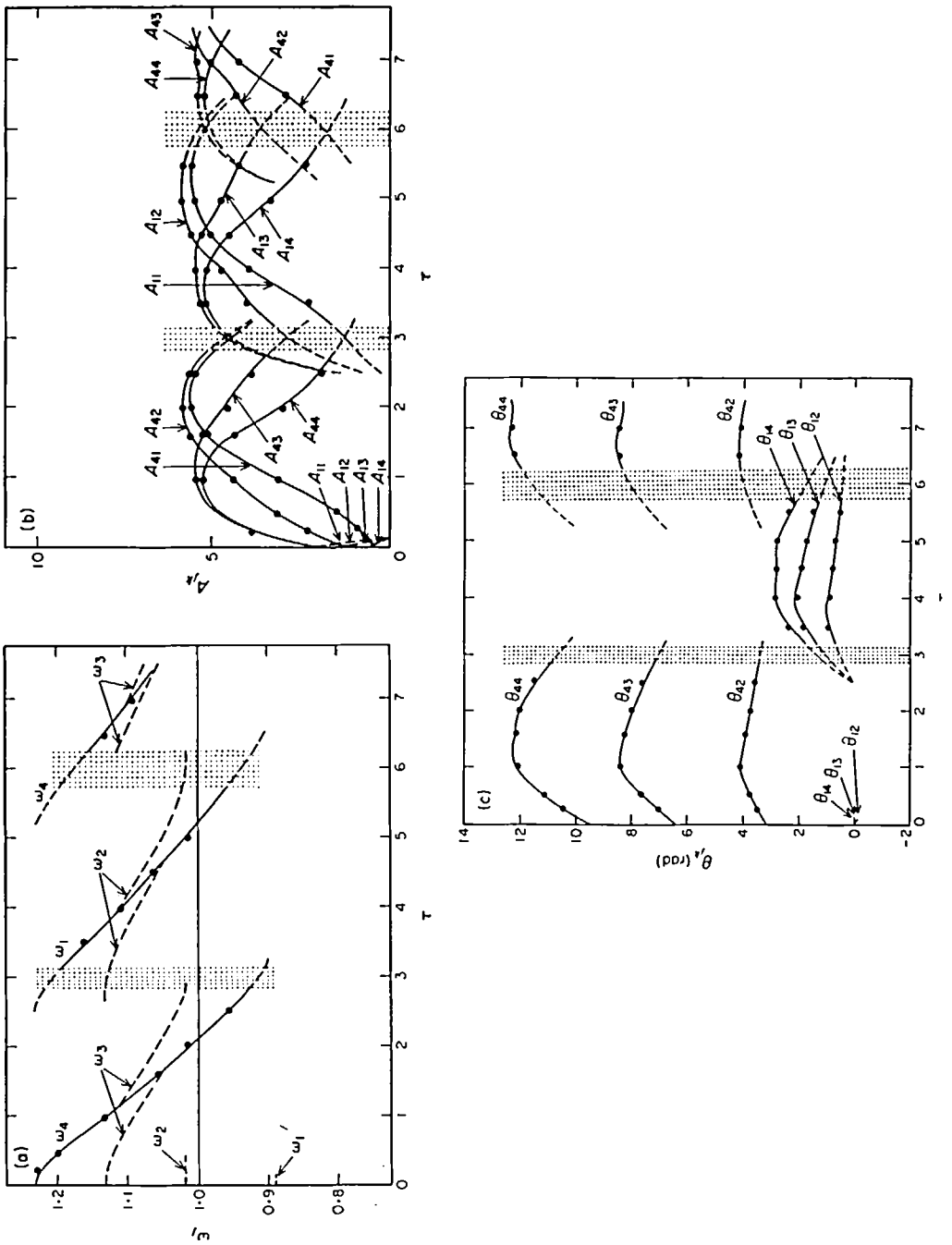
(a)
(b)
(c)
τ
ω_i
A_{jk}
θ_{jk} (rad)
ω_1
ω_2
ω_3
ω_4
A_{11} A_{12} A_{13} A_{14}
A_{41} A_{42} A_{43} A_{44}
θ_{12} θ_{13} θ_{14}
θ_{42} θ_{43} θ_{44}

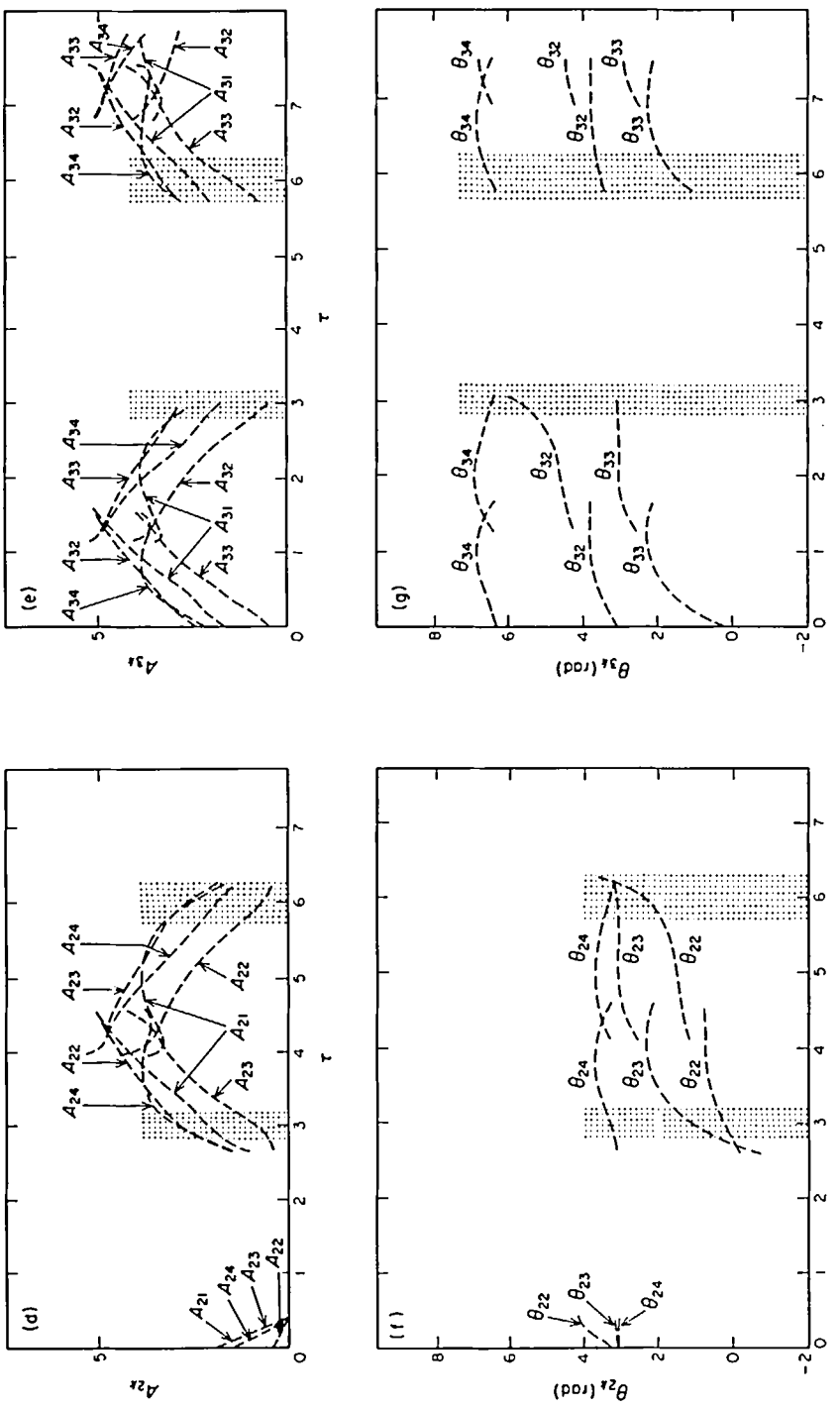

Figure 7. Variations of the entrained frequencies ω_j, entrained amplitudes A_{jk}, and entrained phases θ_{jk} with time delay for $\Delta\omega = 0{\cdot}05$ and $\alpha = 0{\cdot}2$. Note: In the dotted areas of time delay, all the entrained oscillations are unstable. (a) ω_j of mode 1, mode 2, mode 3, and mode 4; (b) A_{jk} of mode 1 and mode 4; (c) θ_{jk} of mode 1 and mode 4 ($\theta_{11} = \theta_{41} = 0$); (d) A_{2k} of mode 2; (e) A_{3k} of mode 3; (f) θ_{2k} of mode 2 ($\theta_{21} = 0$); (g) θ_{3k} of mode 3 ($\theta_{31} = 0$).

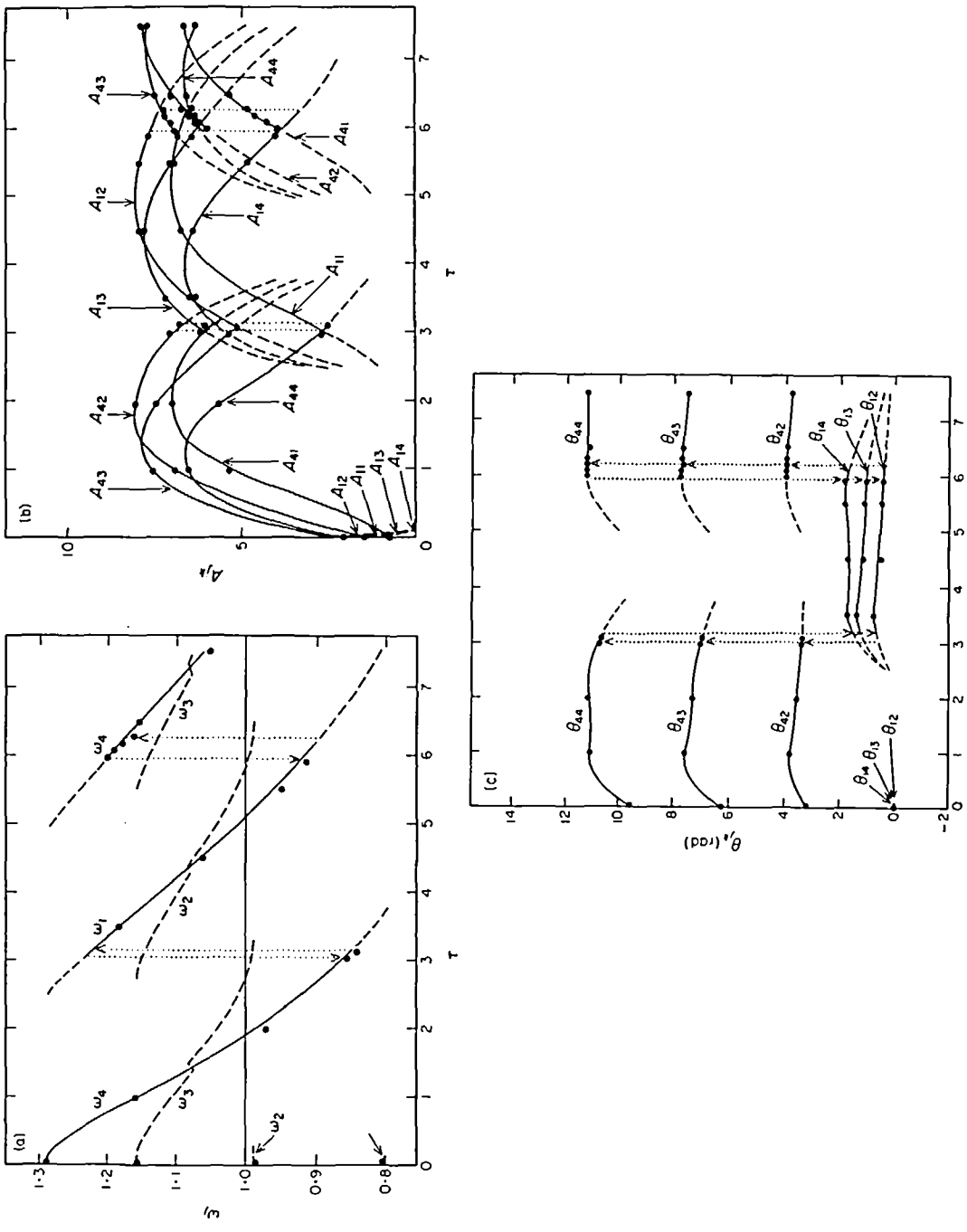
(a)
(b)
(c)
τ
ω_i
A_jk
θ_jk (rad)
ω1
ω2
ω3
ω4
A11
A12
A13
A14
A41
A42
A43
A44
θ11
θ12
θ13
θ14
θ41
θ42
θ43
θ44

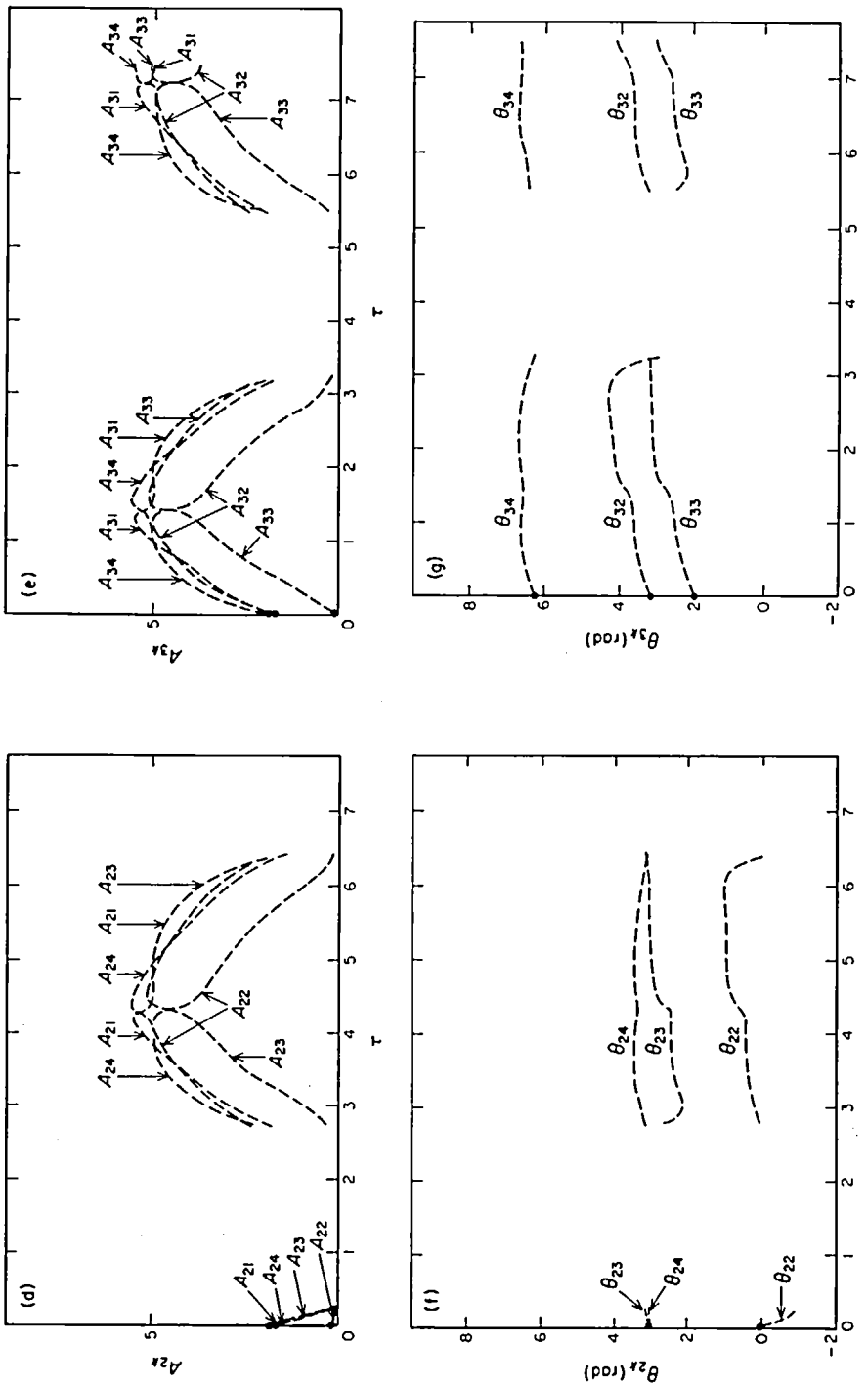

Figure 8. Variations of the entrained frequencies ω_j, entrained amplitudes A_{jk}, and entrained phases θ_{jk} with time delay for $\Delta\omega = 0{\cdot}05$ and $\alpha = 0{\cdot}3$. (a) ω_j of mode 1, mode 2, mode 3, and mode 4; (b) A_{jk} of mode 1 and mode 4; (c) θ_{jk} of mode 1 and mode 4 ($\theta_{11} = \theta_{41} = 0$); (d) A_{2k} of mode 2; (e) A_{3k} of mode 3; (f) θ_{2k} of mode 2 ($\theta_{21} = 0$); (g) θ_{3k} of mode 3 ($\theta_{31} = 0$).

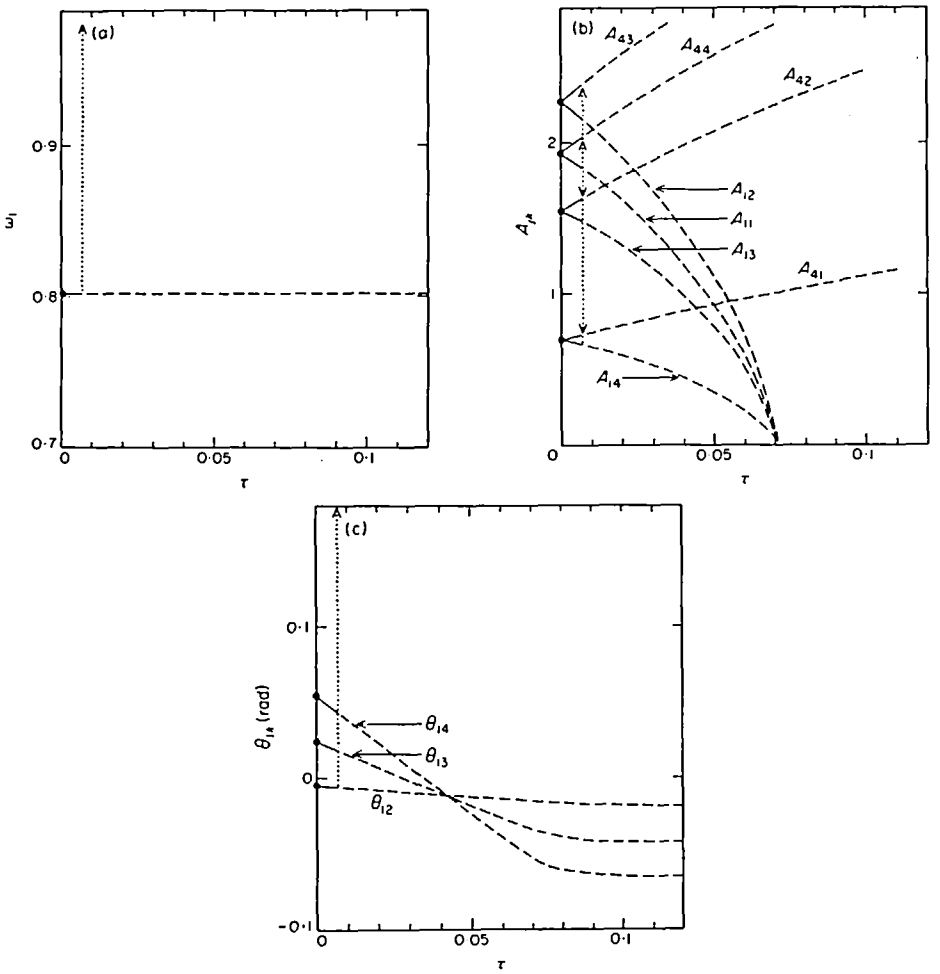

Figure 9. Expanded version of Figure 8 showing mode 1 for very small values of time delay. (a) Entrained frequency; (b) entrained amplitudes (A_{4k} are the entrained amplitudes of mode 4); (c) entrained phases ($\theta_{11} = 0$).

TABLE 1

The stability of four modes of entrained oscillation for sufficiently small values of τ (the theoretical results for $\Delta\omega = 0$)

Coupling factor α	Mode	Delay time τ 0	0·01	0·02	0·03	0·04	0·05	0·06
0·2	Mode 1	S	S	C	U	U	U	U
	Mode 2	S	S	C	U	U	U	U
	Mode 3	S	S	S	S	S	S	U
	Mode 4	S	S	S	S	S	S	S
0·3	Mode 1	S	S	U	U	U	U	U
	Mode 2	S	S	U	U	U	U	U
	Mode 3	S	S	S	S	U	U	U
	Mode 4	S	S	S	S	S	S	S

Note: S, stable; U, unstable; C, critical.

TABLE 2

The stability of four modes of entrained oscillation for sufficiently small values of τ (the theoretical results for $\Delta\omega = 0{\cdot}05$)

Coupling factor α	Mode	Delay time τ 0	0·01	0·02	0·03	0·04
0·2	Mode 1	U	U	U	U	U
	Mode 2	U	U	U	U	U
	Mode 3	U	U	U	U	U
	Mode 4	U	U	S	S	S
0·3	Mode 1	S	U	U	U	U
	Mode 2	S	S	U	U	U
	Mode 3	S	S	S	U	U
	Mode 4	S	S	S	S	S

Note: S, stable; U, unstable.

TABLE 3

Comparison of the theoretical results with results obtained by numerical integration ($\Delta\omega = 0{\cdot}05$, $\alpha = 0{\cdot}2$, and $\tau = 5{\cdot}6$)

Theoretical results			
Oscillator no. k	Entrained frequency ω_1	Entrained amplitude A_{1k}	Entrained phase (rad) θ_{1k}
1	0·971	5·603	0
2		5·811	0·453
3		4·204	1·316
4		2·220	2·140
Results obtained by numerical integration			
Oscillator no. k	Entrained frequency ω_1	Entrained amplitude A_{1k}	Entrained phase (rad) θ_{1k}
1	0·97	5·60	0
2		5·79	0·46
3		4·13	1·36
4		2·16	2·20

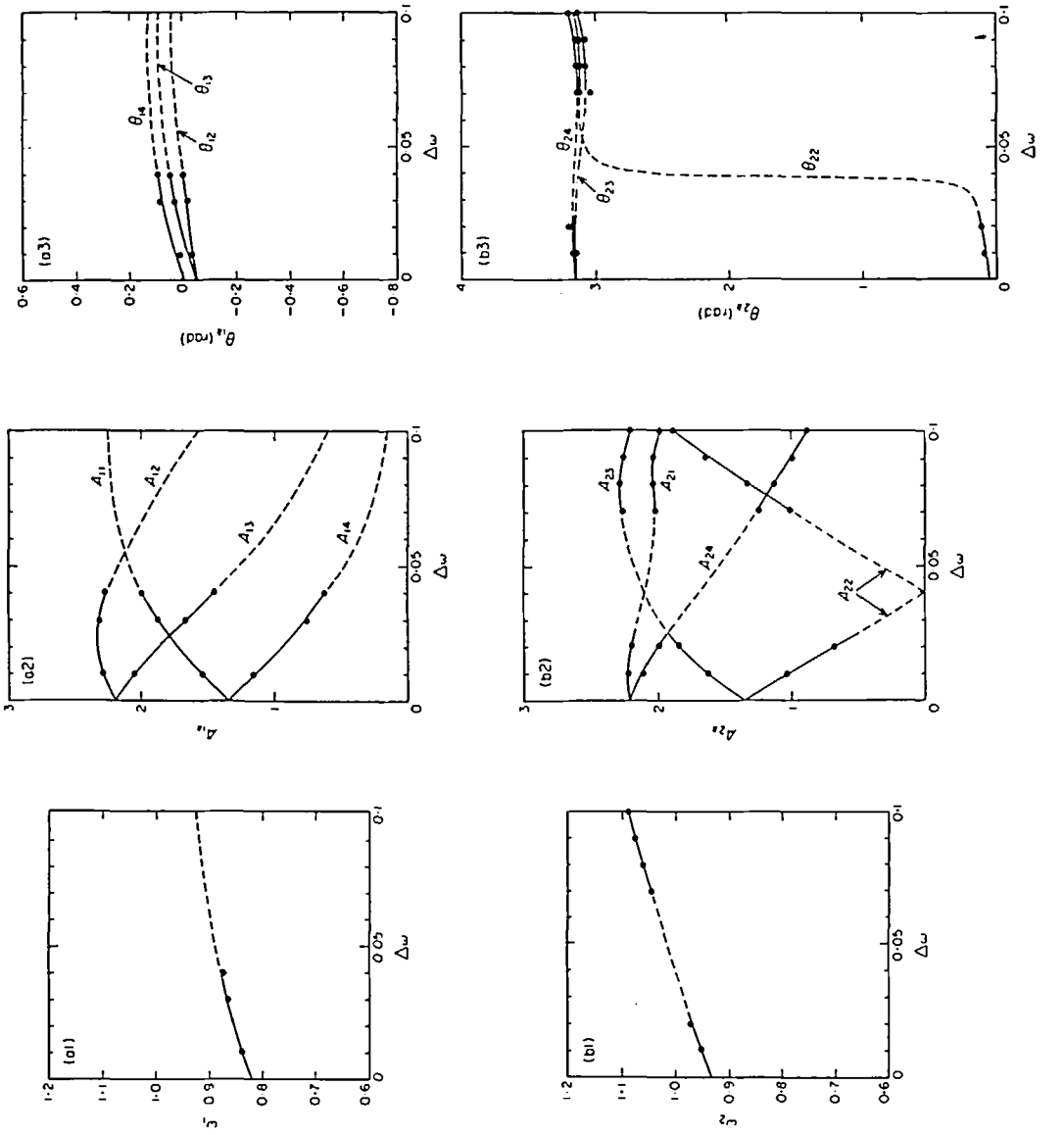
(a1)
(a2)
(a3)
(b1)
(b2)
(b3)
Δω
ζ
A_{1s}
A_{2s}
θ_{1s} (rad)
θ_{2s} (rad)
A_{11}
A_{12}
A_{13}
A_{14}
A_{21}
A_{22}
A_{23}
A_{24}
θ_{11}
θ_{12}
θ_{13}
θ_{14}
θ_{21}
θ_{22}
θ_{23}
θ_{24}

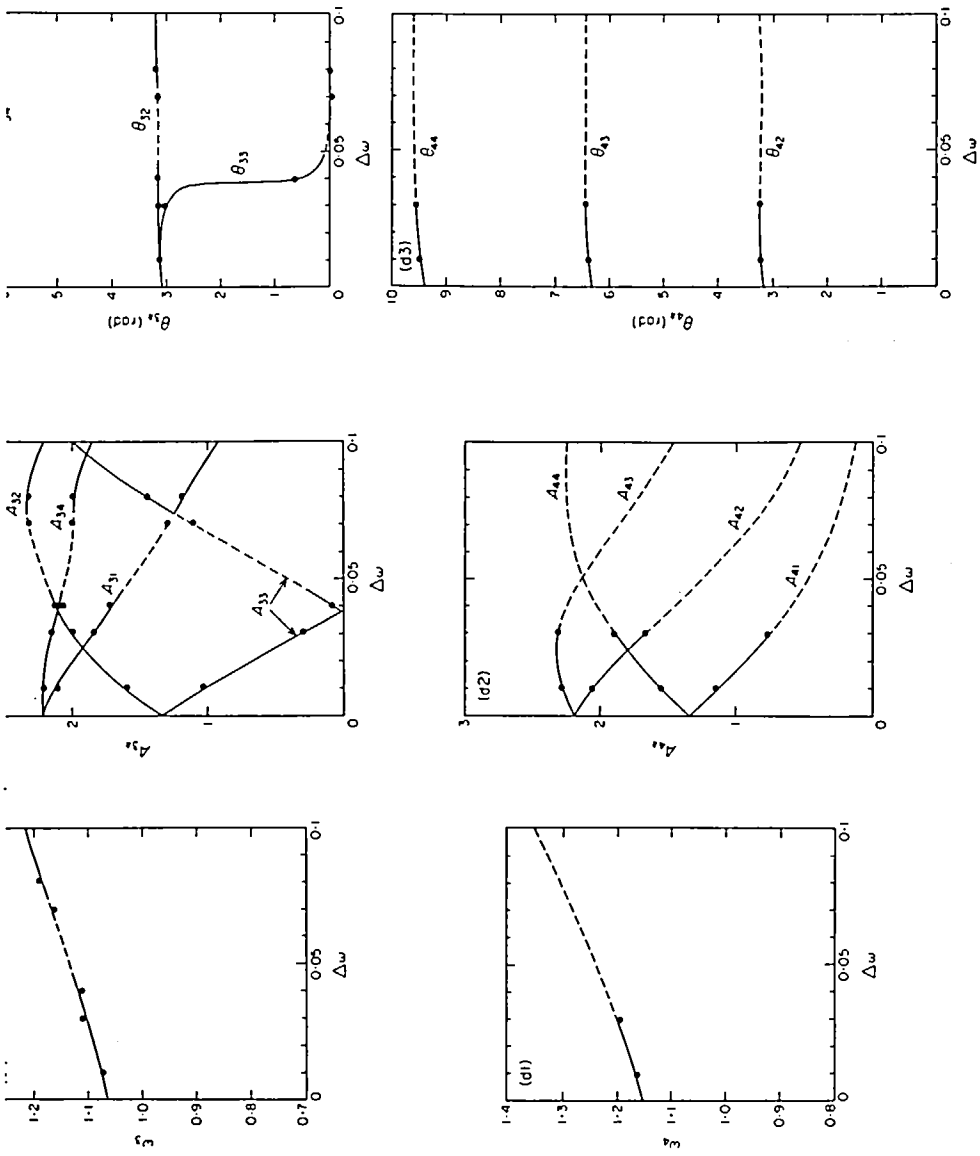

Figure 10. Variations of the entrained frequencies ω_j, entrained amplitudes A_{jk}, and entrained phases θ_{jk} with intrinsic frequency gradient for $\alpha = 0{\cdot}2$ and $\tau = 0$. (a1) Entrained frequency of mode 1; (a2) entrained amplitudes of mode 1; (a3) entrained phases of mode 1 ($\theta_{11} = 0$); (b1) entrained frequency of mode 2; (b2) entrained amplitudes of mode 2; (b3) entrained phases of mode 2 ($\theta_{21} = 0$); (c1) entrained frequency of mode 3; (c2) entrained amplitudes of mode 3; (c3) entrained phases of mode 3 ($\theta_{31} = 0$); (d1) entrained frequency of mode 4; (d2) entrained amplitudes of mode 4; (d3) entrained phases of mode 4 ($\theta_{41} = 0$).

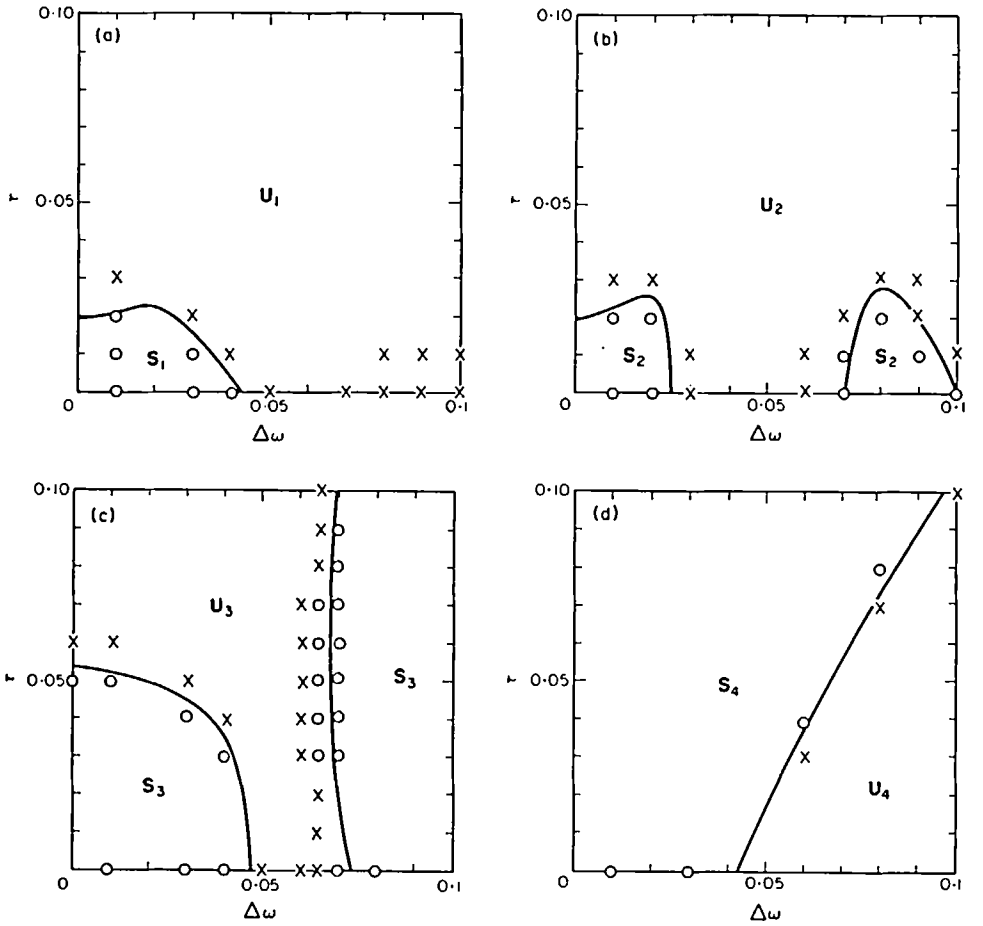

Figure 11. Regions of mode stability for varying time delay and intrinsic frequency gradient ($\alpha = 0{\cdot}2$). Note: In this and following graphs, O, indicate stable modes and ×, indicate unstable modes (O and × are the results obtained by numerical integration). S_k ($k = 1, 2, 3$, and 4) indicate regions of stable mode and U_k ($k = 1, 2, 3$, and 4) indicate regions of unstable mode. (a) Mode 1; (b) mode 2; (c) mode 3; (d) mode 4.

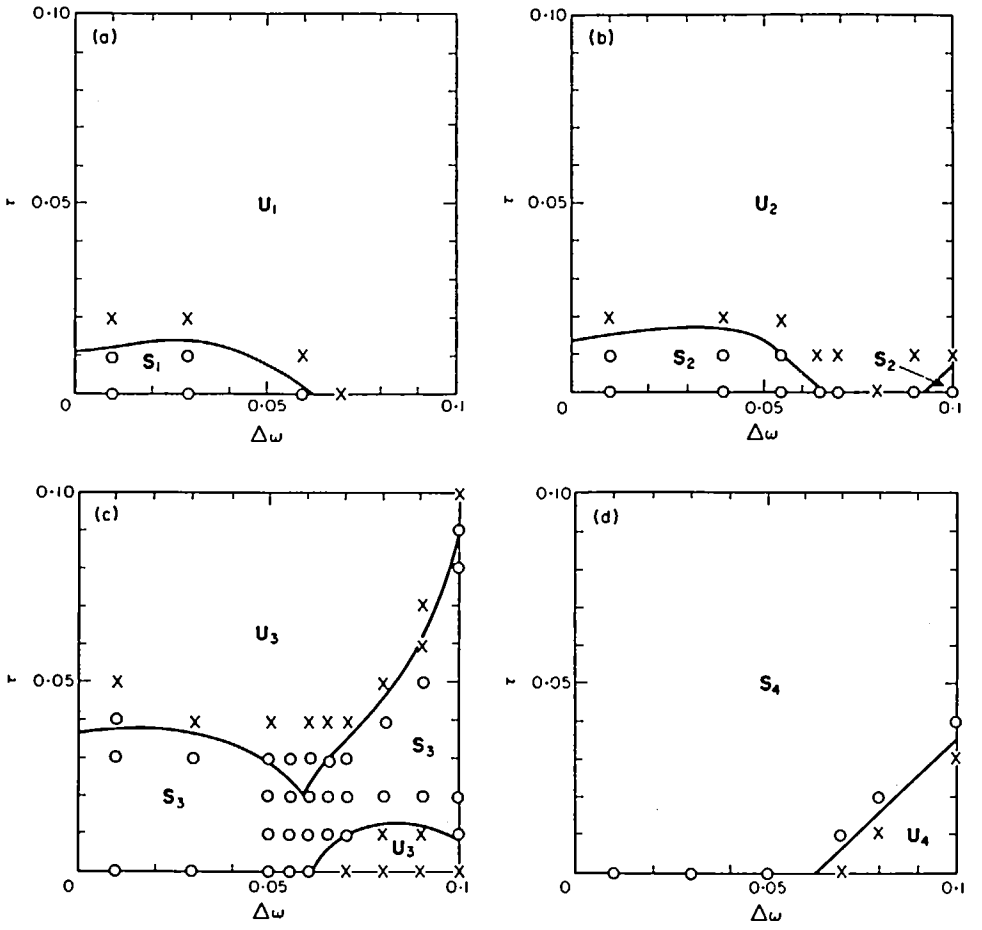

Figure 12. Regions of mode stability for varying time delay and intrinsic frequency gradient ($\alpha = 0{\cdot}3$). (a) Mode 1; (b) mode 2; (c) mode 3; (d) mode 4.

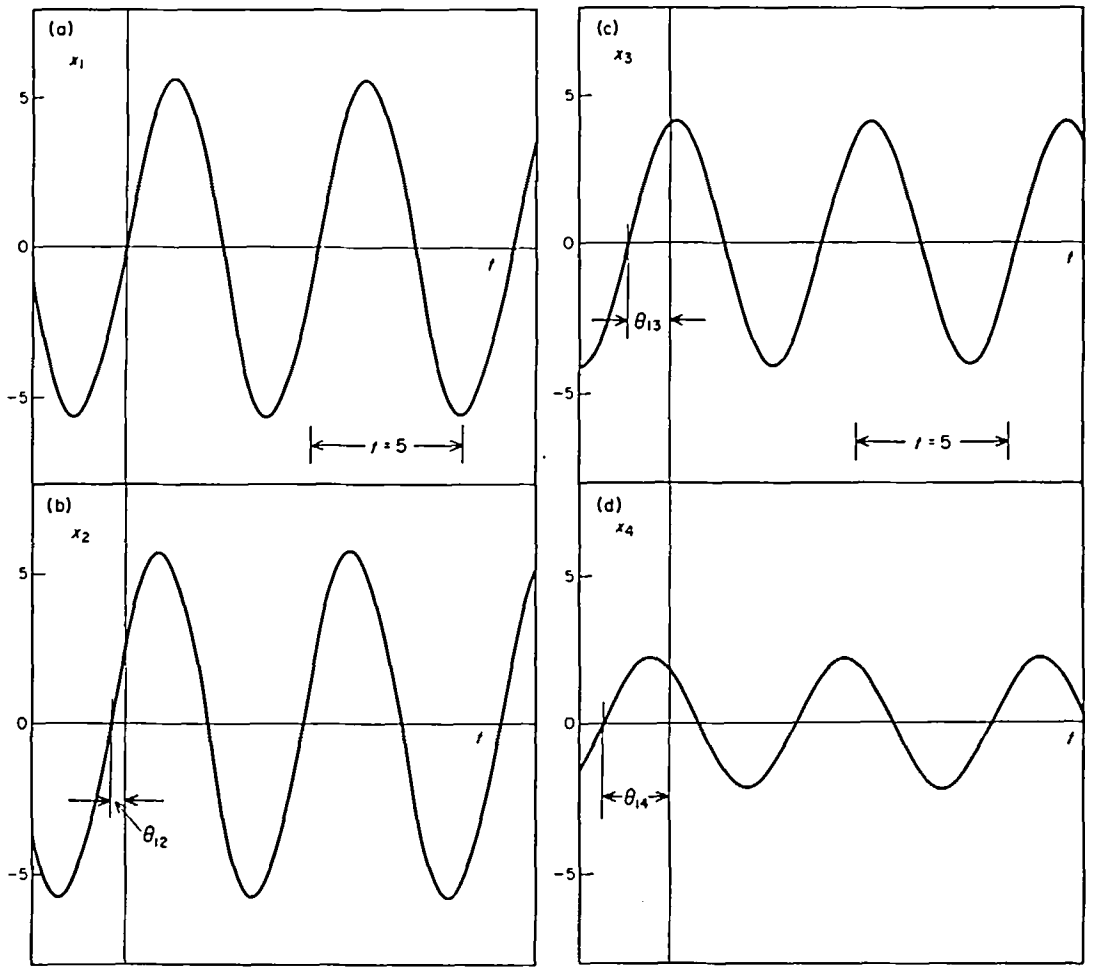

Figure 13. Results obtained by numerical integration ($\Delta\omega = 0{\cdot}05$, $\alpha = 0{\cdot}2$ and $\tau = 5{\cdot}6$). (a) Waveform of x_1; (b) waveform of x_2; (c) waveform of x_3; (d) waveform of x_4.

2 and mode 3 (i.e., A_{22}, θ_{22}, A_{33} and θ_{33}) change appreciably in the neighbourhood of $\Delta\omega = 0{\cdot}04$ as $\Delta\omega$ varies. For very small values of $\Delta\omega$, these modes are stable. As $\Delta\omega$ increases these modes become unstable and then again become stable. The regions of mode stability for varying time delay (very small values) and intrinsic frequency gradient were also obtained, and are shown in Figures 11 and 12.

These theoretical results agree well with those obtained by numerical integration of equation (1) performed with respect to time with the fourth order Runge-Kutta algorithm modified to take delay into account [24],† as shown in Figures 3-12. For $\Delta\omega = 0{\cdot}05$, $\alpha = 0{\cdot}2$, and $\tau = 5{\cdot}6$ the results obtained by numerical integration are given in Figure 13 and Table 3.

† This method was used for the step-size $h = 0{\cdot}01$ ($t_N = Nh + t_0$, $N = 1, 2, 3, \ldots$), and reasonable solutions were obtained.

4. CONCLUSION

A system of four mutually coupled van der Pol oscillators with time delay in the coupling paths has been analyzed. The intrinsic (i.e., uncoupled) frequencies of these oscillators were given by $\omega_{0k} = 1 + \Delta\omega(k-1)$, $k = 1, 2, 3, 4$, where k denotes the four oscillators and $\Delta\omega$ is the intrinsic frequency gradient. The theoretical results obtained have been checked against the digital simulation studies.

It became clear from the results obtained that the coupling time delay, coupling factor, and gradient of intrinsic frequencies radically affect the number, frequency, amplitudes, and phases of entrained oscillations.

For small values of $\Delta\omega$, mode 1 and mode 4 can be interpreted as being an in-phase mode and an anti-phase mode, respectively. Comparing the results with those for a three-oscillator system (see the Appendix) shows that the regions of τ for which the in-phase mode and the anti-phase mode are stable decrease as the number of oscillators and the value of $\Delta\omega$ increase.

It is possible to obtain the in-phase mode with an entrained frequency higher than for the uncoupled condition by suitable choice of time delay. In biological applications, this is one of the phenomena recorded from the small intestine [9]. Hence, system (1) may be used as a subunit of a larger model in intestinal modeling.

In this paper, the four-oscillator system was considered. Both theoretical and experimental studies for systems of more than four oscillators will be reported at a later date.

ACKNOWLEDGMENT

One of the authors (A.K.) would like to thank Professor C. Murase of the Tokyo University of Agriculture and Technology, Tokyo, Japan, for his helpful suggestions.

REFERENCES

1. I. I. BLECKMAN 1971 *Synchronization of Dynamical Systems.* Moscow: Nauka.
2. T. PAVLIDIS 1973 *Biological Oscillators; Their Mathematical Analysis.* New York: Academic Press.
3. T. ENDO and S. MORI 1976 *Transactions of the Institute of Electrical and Electronic Engineers Circuits Systems* **CAS23**, 110-113. Mode analysis of a multimode ladder oscillator.
4. T. ENDO and S. MORI 1976 *Transactions of the Institute of Electrical and Electronic Engineers Circuits Systems* **CAS23**, 517-530. Mode analysis of a two-dimensional low-pass multimode oscillator.
5. T. ENDO and S. MORI 1978 *Transactions of the Institute of Electrical and Electronic Engineers Circuits Systems* **CAS25**, 7-18. Mode analysis of a ring of a large number of mutually coupled van der Pol oscillators.
6. T. ENDO and T. OHTA 1980 *Transactions of the Institute of Electrical and Electronic Engineers Circuits Systems* **CAS27**, 277-283. Multimode oscillations in a coupled oscillator system with fifth-power nonlinear characteristics.
7. D. A. LINKENS 1974 *Transactions of the Institute of Electrical and Electronic Engineers Circuits Systems* **CAS21**, 294-300. Analytical solution of large numbers of mutually coupled nearly sinusoidal oscillators.
8. D. A. LINKENS 1976 *Transactions of the Institute of Electrical and Electronic Engineers Circuits Systems* **CAS23**, 113-121. Stability of entrainment conditions for a particular form of mutually coupled Van der Pol oscillators.
9. D. A. LINKENS 1977 *Bulletin of Mathematics and Biology* **39**, 359-372. The stability of entrainment conditions for RLC coupled van der Pol oscillators used as a model for intestinal electrical rhythms.
10. S. P. DATARDINA and D. A. LINKENS 1978 *Transactions of the Institute of Electrical and Electronic Engineers Circuits Systems* **CAS25**, 308-315. Multimode oscillations in mutually coupled van der Pol type oscillators with fifth-power nonlinear characteristics.

11. N. E. DIAMAT, P. K. ROSE and E. J. DAVISON 1970 *American Journal of Physiology* **219**, 1684-1690. Computer simulation of intestinal slow-wave frequency gradient.
12. S. K. SARNA, E. E. DANIEL and Y. J. KINGMA 1971 *American Journal of Physiology* **221**, 166-175. Simulation of slow-wave electrical activity of small intestine.
13. B. H. BROWN, H. L. DUTHIE, A. R. HORN and R. H. SMALLWOOD 1957 *American Journal of Physiology* **229**, 384-388. A linked oscillator model of electrical activity of human small intestine.
14. V. P. RUBANIK 1969 *Oscillation of Quasilinear Systems with Retardations.* Moscow: Nauka.
15. Y. I. MARCHENKO 1967 *Radiofizika* **10**, 1533-1539. Inter-synchronization of the auto-oscillating system with the account of interaction forces time delay.
16. A. KOUDA and S. MORI 1981 *Transactions of the Institute of Electrical and Electronic Engineers Circuits Systems* **CAS28**, 247-253. Analysis of a ring of mutually coupled van der Pol oscillators with coupling delay.
17. A. KOUDA and S. MORI 1982 *International Journal of Non-linear Mechanics* **17**, 267-276. Mode analysis of a system of mutually coupled van der Pol oscillators with coupling delay.
18. J. GRASMAN and M. J. W. JANSEN 1979 *Journal of Mathematics and Biology* **7**, 171-197. Mutually synchronized relaxation oscillations as prototypes of oscillating systems in biology.
19. D. A. LINKENS and R. I. KITNEY 1982 *Bulletin of Mathematics and Biology* **44**, 57-74. Mode analysis of physiological oscillators intercoupled via pure time delays.
20. C. HAYASHI 1964 *Nonlinear Oscillations in Physical Systems.* New York: McGraw-Hill.
21. B. C. KUO 1962 *Automatic Control Systems.* Englewood Cliffs, New Jersey: Prentice-Hall.
22. A. M. OSTROWSKI 1960 *Solution of Equations and Systems of Equations.* London: Academic Press, second edition, 1966 re-issue.
23. A. D. BOOTH 1955 *Numerical Methods.* London: Butterworth. Japanese translation 1968 K. Udagawa and G. Nakamura, Tokyo: Corona Publishing Co., Ltd.
24. S. D. CONTE and C. D. BOOR 1981 *Elementary Numerical Analysis—An Algorithmic Approach.* New York: McGraw-Hill, third edition.

APPENDIX

A three-oscillator system described by the following equations has been studied:

$$\ddot{x}_1 - \varepsilon(1-x_1^2)\dot{x}_1 + \omega_{01}^2 x_1 = \alpha x_2(t-\tau),$$

$$\ddot{x}_2 - \varepsilon(1-x_2^2)\dot{x}_2 + \omega_{02}^2 x_2 = \alpha \dot{x}_1(t-\tau) + \alpha x_3(t-\tau),$$

$$\ddot{x}_3 - \varepsilon(1-x_3^2)\dot{x}_3 + \omega_{03}^2 x_3 = \alpha x_2(t-\tau). \qquad \text{(A1)}$$

Here dots represent differentiation with respect to time, x_k $(k = 1, 2, 3, 4)$ is the output of the kth van der Pol oscillator, ω_{0k} $(= 1 + \Delta\omega(k-1))$ is the intrinsic frequency of that oscillator, $\Delta\omega$ is the intrinsic frequency gradient, ε is the waveshape parameter, α is the coupling factor, and τ is the delay time.

A numerical analysis was carried out for a waveshape parameter of 0·03, a coupling factor of 0·2, and intrinsic frequency gradients of zero and 0·05.

In this system, there are three modes of entrained oscillation. The results are shown in Figures A1-A3. As shown in these figures, the results for mode 1 and mode 3 are similar to those for mode 1 and mode 4 of the four-oscillator system, respectively (see Figures 3-12). Mode 2 is unstable for very small values of $\Delta\omega$. This mode becomes stable and then again becomes unstable as $\Delta\omega$ increases (the stable mode 2 becomes unstable as τ is increased from zero).

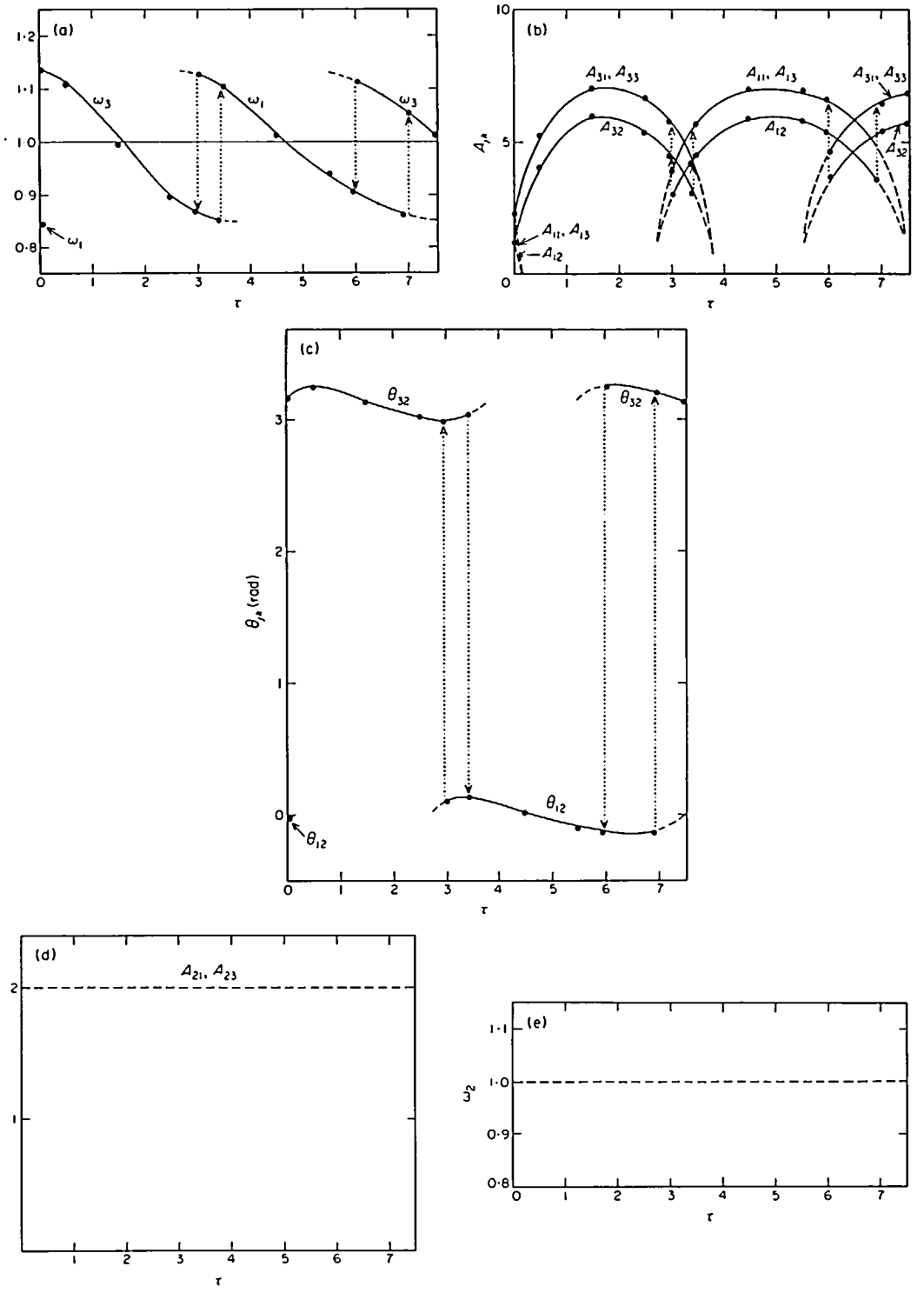

Figure A1. Variations of the entrained frequencies ω_j, entrained amplitudes A_{jk}, and entrained phases θ_{jk} with time delay for $\Delta\omega = 0$. (a) ω_j of mode 1 and mode 3; (b) A_{jk} of mode 1 and mode 3; (c) θ_{jk} of mode 1 and mode 3 ($\theta_{11} = \theta_{31} = 0$, $\theta_{13} = 0$, and $\theta_{33} = 2\pi$); (d) ω_2 of mode 2; (e) A_{2k} of mode 2 ($A_{22} = 0$); θ_{22} is arbitrary ($\theta_{21} = 0$ and $\theta_{23} = \pi$).

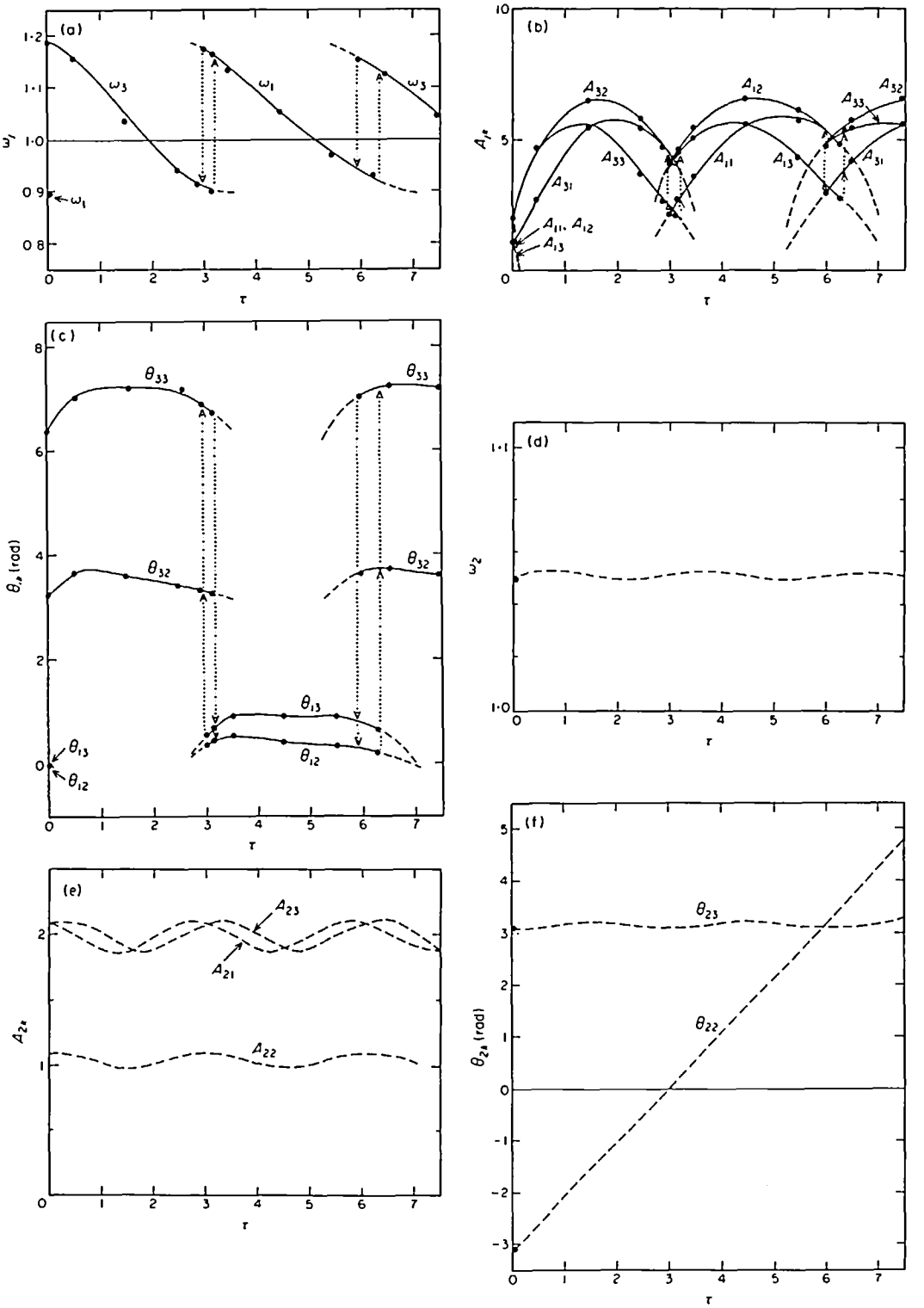

Figure A2. Variations of the entrained frequencies ω_j, entrained amplitudes A_{jk}, and entrained phases θ_{jk} with time delay for $\Delta\omega = 0{\cdot}05$. (a) ω_j of mode 1 and mode 3; (b) A_{jk} of mode 1 and mode 3; (c) θ_{jk} of mode 1 and mode 3 ($\theta_{11} = \theta_{31} = 0$); (d) ω_2 of mode 2; (e) A_{2k} of mode 2; (f) θ_{2k} of mode 2 ($\theta_{21} = 0$).

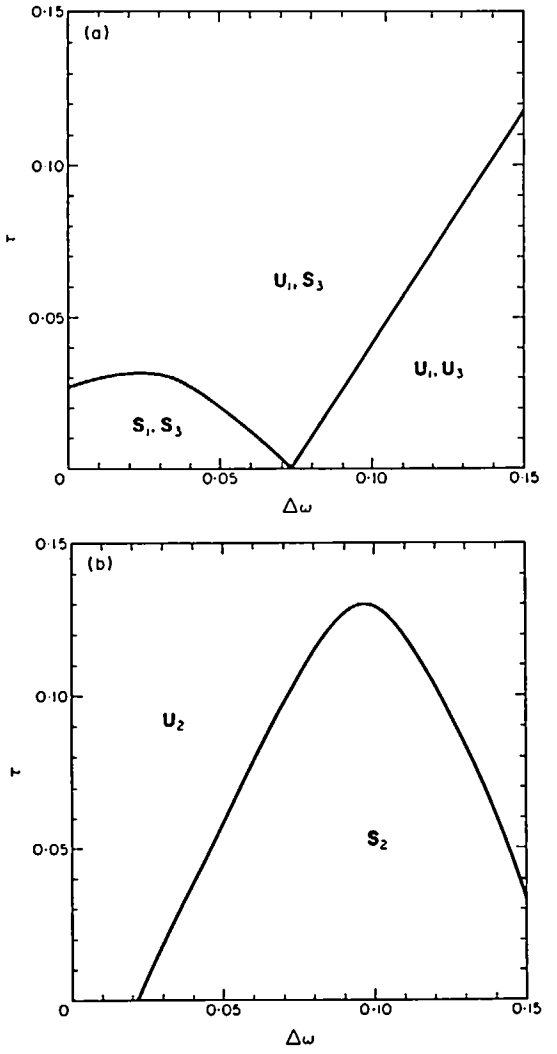

Figure A3. Regions of mode stability for varying time delay and intrinsic frequency gradient. Note: S_k ($k = 1$, 2, and 3) indicate regions of stable modes and U_k ($k = 1$, 2, and 3) indicate regions of unstable modes. (a) Mode 1 and mode 3; (b) mode 2.